Electrical breakdown in low pressure gases

2002 J. Phys. D: Appl. Phys. 35 R91

(http://iopscience.iop.org/0022-3727/35/10/201)

INSTITUTE OF PHYSICS PUBLISHING JOURNAL OF PHYSICS D: APPLIED PHYSICS

J. Phys. D: Appl. Phys. **35** (2002) R91–R103 PII: S0022-3727(02)23795-X

TOPICAL REVIEW

Electrical breakdown in low pressure gases

Momčilo M Pejović[1], **Goran S Ristić**[1,2] **and Jugoslav P Karamarković**[1,3]

[1] Faculty of Electronic Engineering, University of Niš, Beogradska 14, 18000 Niš, Serbia, Yugoslavia

[2] Current address: Department of Medical Biophysics and Medical Imaging, University of Toronto, Sunnybrook Health Science Centre, 2075 Bayview Avenue, Toronto, Ontario, Canada M4N 3M5

[3] Also at: Faculty of Civil Engineering and Architecture, University of Niš, Beogradska 14, 18000 Niš, Serbia, Yugoslavia

E-mail: pejovic@elfak.ni.ac.yu

Received 2 January 2002
Published 30 April 2002
Online at stacks.iop.org/JPhysD/35/R91

Abstract

The paper presents the results of investigation of the electrical breakdown in low pressure gases when the secondary electrons released from the cathode play the dominant role in the initiation of electrical breakdown. The secondary electrons are created by the charged and neutral species formed during the previous breakdown and discharge as well as by γ-rays. Electrical breakdown investigations are based on the measurements of electrical breakdown voltage and electrical breakdown time delay for gas-filled tubes with spherical electrodes with diameters much larger than an interelectrode distance. Stochastic nature of both the breakdown voltage and time delay are discussed and their distributions based on experimental data are shown. The methods for the determination of static breakdown voltage are also analysed. The influence of different parameters (overvoltage, cathode material and its surface purity, gas pressure, glow current, etc) on time delay are studied. A special attention is paid to the memory effect in various gases that depends on the positive ion recombination times, catalytic recombination times in the case of nitrogen and hydrogen, as well as metastable states deexcitation times in noble gases. The analysis of this effect is done by memory curves on the basis of which the presence of long-lived neutral active states can be followed to their very low concentrations when cosmic and environment radiation play the dominant role in electrical breakdown initiation.

1. Introduction

The importance of the research of physical processes that initiate electrical breakdown, generating the low temperature plasma in various gases at low pressures, lays in numerous gas applications. Controlled electrical breakdown is very important in pulsed power applications and represents the basis of the operation of gas-filled switches in fusion reactors, lasers, directed-energy weapons, and electromagnetic pulse generators. The other gas applications lay in various technologies, including thin film deposition, semiconductor processing, materials treatment (modification of surface physics and surface chemistry, sterilization), lamps, light sources and displays, thick film deposition, waste treatment and materials analysis. Gases are also used as insulation to prevent breakdown in high-voltage circuits and transmission lines.

The most common method for producing the electrical

breakdown, generating and sustaining of a low temperature plasma, is applying high electric field to a neutral gas. Any volume of neutral gas always contains a few electrons and ions that are, for example, the result of the interaction of cosmic rays or environment radiation with the gas atoms. These free charge carriers are accelerated by the electric field, colliding with atoms/molecules in the gas and with the electrode surfaces, and new charged particles may be created. This leads to an avalanche of charged particles and to the initiation of electrical breakdown in the gas. The electrical breakdown is characterized by the rapid gas transition from a very poor electrical conductor with the resistivity of $\approx 10^{14}\ \Omega\,\mathrm{m}$ to a relatively good conductor with a resistivity that is many orders of magnitude lower (the resistivity depends on particular conditions and is typically about $10^{3}\ \Omega\,\mathrm{m}$ in glow discharge) [1]. The ionized states produced in the gas by electrical breakdown build up in a time which varies from 10^{-9} s to several seconds, although usually it is between 10^{-8} and 10^{-4} s [1].

During the electrical breakdown and later discharge processes, the charged and neutral active species are created. Their initial concentrations depend on the pressure and gas type in the tube, glow current, glow time, etc. After the discharge has been ceased, these species recombine or deexcite in the gas volume, on tube walls and electrodes. The recombination and deexcitation processes on the cathode can release secondary electrons, which are very important for a subsequent breakdown [2]. The concentrations of these species depend on the time elapsed from a voltage turn-off to the next voltage turn-on, and this time interval is known as an afterglow period (relaxation time) τ.

The aim of this paper is to present a review of some of our previous published results, as well as to show some new results relating to the electrical breakdown in gases at low pressures, including the analysis of physical processes which initiate electrical breakdown in gases using time delay versus afterglow period measurements. The method is proposed for the detection of charged and neutral active species, formed during breakdown and later discharge, to their very low concentration, when other known methods cannot be applied. The analysis of the methods for gas tube static breakdown voltage determinations is also performed.

2. Theory of the electrical breakdown

2.1. Non-self-sustaining discharge and breakdown

If the voltage lower than breakdown voltage U_b is applied to the gas tube, there will be no current response. However, if some ionization source (such as UV-, x- or γ-rays) is applied to the interelectrode space, or if the cathode is heated, the charge carriers (electrons and ions) will be formed in the interelectrode space and their drift will produce an electric current in the tube. If the external ionization source is removed, the current in the tube vanishes. The increase of applied voltage, with permanent presence of an external ionization source, initially leads to the increase of the current followed by current saturation [3]. Further increase of voltage gives the electrons sufficient kinetic energy to induce the ionization of neutral particles in the collisions with them, causing further increase of the current [4]. The positive ions also obtain kinetic energy sufficient to release the electrons from the cathode in the so-called secondary emission process. The secondary electron emissions (SEE) from the cathode can be produced not only by positive ions, but also by neutral active states created during previous breakdown and discharge. The number of the electrons that reach anode N_a can be expressed following Townsend theory as [5]:

$$N_\mathrm{a} = N_0 \frac{\exp(\alpha d)}{1 - \gamma[\exp(\alpha d) - 1]}, \tag{1}$$

where N_0 is the number of the electrons created by external ionization source, d is the interelectrode distance, and α is the first Townsend's coefficient which depends on the gas type and gas pressure p, as well as on the electric field in the interelectrode space E [6]:

$$\alpha = Ap \exp\left(-\frac{Bp}{E}\right), \tag{2}$$

where the constants A and B are different for different gases. The parameter γ in equation (1) is secondary emission coefficient that depends on cathode material and gas type, as well as on the ratio E/p [6].

Ionization processes in the interelectrode space and SEE cause rapid increase of the current, producing the transformation of non-self-sustaining discharge to some form of self-sustaining discharge. This phenomenon is known as electrical breakdown.

2.2. Electrical breakdown probability

When the electric field in the interelectrode space E is sufficiently high to create the multiplication of the electrons and ions, the avalanche appears. If this multiplication creates a sufficient number of electrons and ions, it will lead to the electrical breakdown. However, if the processes of free charge species losses are emphasized, the avalanche multiplication can cease [7]. Due to the statistical nature of both creation and loss of free species, breakdown may not occur even if applied voltage U_w is higher than the breakdown voltage U_b. The statistical treatment of electrical breakdown in gas started with statistical theory of Zuber [7] and von Laue [8], which was further developed in the investigations of Loeb [9] and Wijsman [10]. On the basis of statistical theory, 'an initial electron' is required for the formation of electrical breakdown, but it does not mean that electrical breakdown will definitely occur if an initial electron appears. The probability of this event, W, is known as breakdown probability and it depends on the existing conditions in the tube. This probability (different for every created electron) is a complicated function of electron position, electric field, gas pressure and Townsend coefficients α and γ [11, 12]. However, W could be considered as a constant for every electron created at the cathode if a constant and uniform electric field exists in the interelectrode space. The calculations of these probabilities for the gas at low pressure in the case when the secondary electrons are released from the cathode were done by Wijsman [10], neglecting the influence of space charge in the interelectrode space. It was also assumed that all avalanches created by particular

initial electrons are independent, and the mean value of created electrons on path d in the avalanche is $\bar{N} = \exp(\alpha d)$. Thus, in the case of SEE the probability of successful avalanche is

$$W = \begin{cases} 0 & \text{for } q < 1, \\ 1 - \dfrac{1}{q} & \text{for } q \geqslant 1, \end{cases} \tag{3}$$

where $q = \gamma(\bar{N} - 1) = \gamma[\exp(\alpha d) - 1]$. W is the function of electrodes' applied voltage U_w and requires the dependence q on U_w to be calculated [10, 13, 14]. If U_w is lower than breakdown voltage U_b, then $q < 1$, the discharge is non-self-sustaining and the current will flow only in the presence of external ionization source. In the case of $q > 1$, the breakdown probability W becomes

$$W = 1 - \frac{1}{\gamma[\exp(\alpha d) - 1]} \tag{4}$$

2.3. Breakdown condition: Paschen's law

The breakdown condition for the gases at low pressures can be obtained using Townsend's theory represented by equation (1), including the fact that influence of the space charge can be neglected in the early stage of the breakdown. Space charge is needed for the determination of the regime that will be established after the breakdown.

Equation (1) shows that if the denominator tends to zero with $N_0 \neq 0$, then an unlimited current increase will occur. In reality, the current will be limited to some finite value determined by the external circuit. The breakdown condition is [3–5]:

$$\gamma[\exp(\alpha d) - 1] = 1, \tag{5}$$

or

$$\alpha d = \ln\left(1 + \frac{1}{\gamma}\right). \tag{6}$$

It also means that the current can be sustained if the external source of radiation is absent ($N_0 = 0$), i.e. it is self-sustaining discharge. In other words, equation (5) represents a condition for breakdown initiation. Combining (2) and (6), we obtain

$$Apd \exp -\frac{Bp}{E} = \ln\left(1 + \frac{1}{\gamma}\right) \tag{7}$$

If electrodes are planeparallel, $E = U_b/d$, and it follows that

$$U_b = \frac{Bpd}{\ln(Apd) - \ln[\ln(1 + 1/\gamma)]}. \tag{8}$$

Expression (8) is Paschen's law implying that U_b depends only on $p \cdot d$ instead of the particular dependence on the pressure and interelectrode distance.

It is easy to show that for

$$pd = \frac{\exp(1)}{A} \ln\left(1 + \frac{1}{\gamma}\right) \tag{9}$$

U_b has the minimum value

$$U_{b\min} = \exp(1)\frac{B}{A} \ln\left(1 + \frac{1}{\gamma}\right). \tag{10}$$

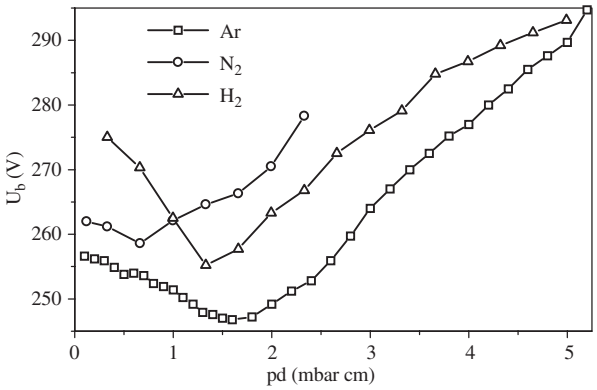

Figure 1. Breakdown voltage U_b in three gases as a function of pd values (Paschen curves).

Many investigations [4–6] confirm that Paschen's curves $U_b = f(pd)$ really have minima. $U_{b\min}$ depends on gas type and cathode material, as well as on their purity.

The investigations performed during last two decades in our laboratories showed [15, 16] that Paschen's curves also exist for gas tubes with spherical electrodes if their diameters are much larger than the interelectrode distances. Our latest results for argon-, nitrogen- and hydrogen-filled tubes are shown in figure 1. The results are obtained in the case of constant pressure (6.7 mbar) and spherical iron electrodes, one fixed and the other movable so that the electrode separation may be continuosly changed by a permanent magnet from outside. Comparison of these results with those obtained for the same gases, but in the case of plane-parallel electrodes [17], shows qualitative agreement.

2.4. Definitions of breakdown voltage and time delay

Electrical breakdown in gases does not take place instantly upon applying a voltage U_b to the electrodes of gas-filled tube, but after a corresponding delay known as electrical breakdown time delay t_d that is mutually dependent on U_b. Due to the statistical nature of processes which initiate breakdown, U_b and t_d are mutually dependent stochastic variables with certain distributions. The distribution function of t_d defines the probability of electrical breakdown in any time interval. Thus, if $f(t)$ is the time delay probability density function (distribution density), then a breakdown occurrence probability in time interval $(t, t + \mathrm{d}t)$ is $f(t)\,\mathrm{d}t$. This probability describes the phenomenon of electrical breakdown in the tube, and should not be mistaken for (de facto microscopic) breakdown probability W from Townsend's theory.

There are several definitions of breakdown voltage in the literature. One of the most commonly used definition states that U_b is the voltage when the gas transits from non-self-sustaining to self-sustaining discharge [5, 6]. On the basis of the statistical theory of electrical breakdown [10], U_b is defined as the highest voltage which keeps breakdown probability W at zero value (see equation (3)), i.e. a voltage on the onset of breakdown condition (equation (5)). Due to the fluctuation of the parameters α and γ with time, the electrical breakdown usually does not occur for the same voltage in a series of experiments. Also, the breakdown voltage depends on the time dependence of the applied voltage.

For each gas tube, it is of a great importance to define the minimum value of the breakdown voltage U_b, i.e. the minimum voltage applied on the tube that still can induce the electrical breakdown. This breakdown voltage value is known as a static breakdown voltage U_s [18], representing one of the most important parameters of the gas-filled tube. The explicit definition of static breakdown voltage is possible using the t_d distribution. Thus, if voltage lower than U_s is applied on the tube, time delay probability density function $f(t)$ will be identically equal to zero for each t, and the probability of electrical breakdown in any finite time interval will be zero, hence t_d will be infinitely long. If the applied voltage U_w exceeds U_s, $f(t)$ will have a non-zero value, and the probability of breakdown in any time interval will exist and can be measured. Thus, the static breakdown voltage U_s can be defined as the highest voltage that can be applied on the tube for which the time delay is still infinite [19].

There are also several more exact definitions of t_d. One of them is as follows: t_d is the time elapsed from the instant of time when applied voltage reaches the breakdown voltage to the moment when it starts to decrease due to the breakdown in gas-filled tube [20]. The other definition [19, 21] states that t_d is the time interval between the moment of U_w ($U_w > U_s$) application on the tube and the moment when the tube current exhibits a detectable discharge.

The t_d consists of the statistical time delay (t_s) and formative time (t_f), i.e. $t_d = t_s + t_f$. The statistical time delay is the period of the time elapsed between the instant of application of U_w ($U_w > U_s$) and the appearance of a free electron that initiates the breakdown process (so-called effective electron) [1]. The time taken from the end of the statistical time delay to the onset of breakdown, characterized by the collapse of the applied voltage as a self-maintained glow, is the formative time [1].

2.5. Distributions of breakdown voltage and time delay

The distribution of time delay depends on the distributions of statistical time delay and formative time, which are different due to the different physical mechanisms that determine these times. t_f is determined by a successful avalanche process and has a distribution with small variance, i.e. $\sigma_{t_f} \ll \bar{t_f}$. Consequently, in the case of given measurement conditions, t_f could be approximated as a deterministic variable characterized by constant value.

t_s is the time needed for an effective electron appearance. The appearance rate z of the effective electrons depends on the appearance rate Y of initial secondary electrons, and breakdown probability W. The secondary electron appearance processes in the vicinity of the cathode can be successfully modelled by Poisson random process. The number of secondary electrons created in the observed time interval $(0, t_1)$ is a random variable with Poisson distribution $\mathcal{P}(\lambda)$, where $\lambda = \int_0^{t_1} Y(t)\,\mathrm{d}t$. If the analysis is restricted to the case of t_1 so small that W can be considered a constant, then $z = YW$ [22]. Thus, following the probability theory, the probability density function $f(t)$ and cumulative distribution function $F(t)$ of a stochastic variable that represents time to the appearance of an effective electron (i.e. statistical time delay) is related with $z(t)$, with

$$z(t) = \frac{f(t)}{1 - F(t)}, \tag{11}$$

leading to

$$f(t) = z(t) \exp\left(-\int_0^t z(t')\,\mathrm{d}t'\right). \tag{12}$$

For constant Y and W, statistical time delay has exponential distribution $\mathcal{E}(YW)$:

$$f(t) = YW \exp[-YWt]. \tag{13}$$

The distribution of total time delay depends on the ratio of t_f and t_s, and three different cases can be considered:

(i) $t_f \gg t_s$. In this case the time delay is effectively only the formative time $t_d \approx t_f$. Physically, it corresponds to the case with very large z, when effective electron is produced immediately.

(ii) $t_f \approx t_s$. The rate of the appearance of effective electrons is smaller and formative time and statistical time are of the same order.

(iii) $t_f \ll t_s$. z is small enough and t_d has the same statistical nature as t_s, i.e. $t_d \approx t_s$.

Analysing the distribution of time delay in case (iii), keeping in mind that $t_d = t_s + t_f$ and assuming deterministic t_f, t_d obeys shifted exponential distribution with a probability density function

$$f(t) = \begin{cases} 0 & \text{for } t < t_f, \\ YW \exp[-YW(t - t_f)] & \text{for } t \geqslant t_f. \end{cases} \tag{14}$$

The cumulative distribution function is defined as the probability that breakdown takes place before the moment of time t

$$F(t) = P\{t_d < t\} = \int_{t_f}^{t} f(t')\,\mathrm{d}t' = 1 - \exp[-YW(t - t_f)], \tag{15}$$

while the probability that breakdown will appear after the moment of time t has the form

$$R(t) \equiv 1 - F(t) = P\{t_d > t\} = \int_t^{+\infty} f(t')\,\mathrm{d}t' = \exp[-YW(t - t_f)]. \tag{16}$$

Mean value $\bar{t_d}$ and standard deviation σ are

$$\bar{t_d} = \int_{t_f}^{+\infty} t f(t)\,\mathrm{d}t = t_f + \frac{1}{YW} = t_f + \bar{t_s}, \tag{17}$$

$$\sigma = \left\{\int_{t_f}^{+\infty} (t - \bar{t_d})^2 f(t)\,\mathrm{d}t\right\}^{1/2} = \frac{1}{YW} = \bar{t_d} - t_f. \tag{18}$$

The distribution of breakdown voltage depends on the time function of applied voltage. If U_w linearly increases from the value lower than U_s, it is possible to write in equation that connects the two stochastic variables U_b and t_d:

$$U_b = U_s + kt_d, \tag{19}$$

where k is the rate of increase of the applied voltage. The probability density function $f(U)$ of breakdown voltage U_b

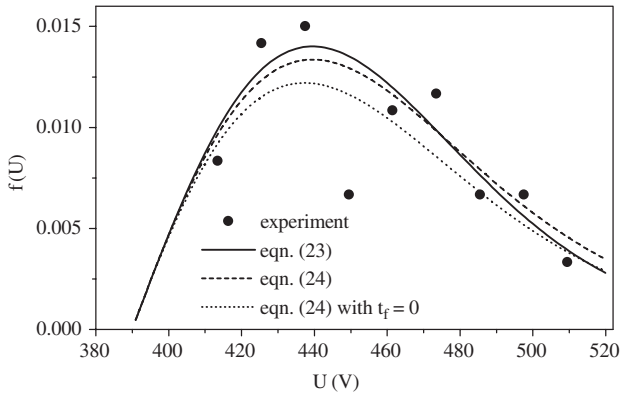

Figure 2. Comparison of probability density functions of breakdown voltage: complete (equation (23)) and simplifed (equation (24)), with $t_f \neq 0$ and $t_f = 0$.

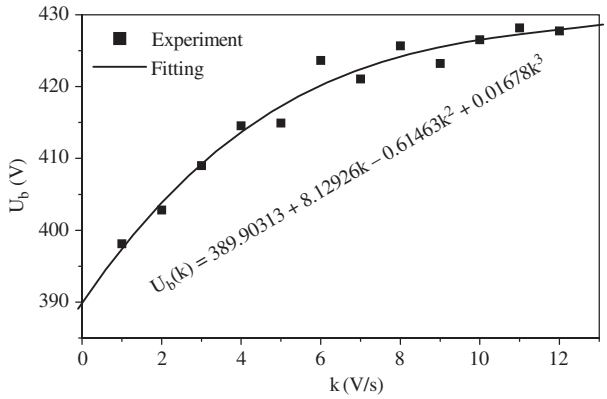

Figure 3. Breakdown voltage U_b as a function of the rate $k = 1$–$12\,\mathrm{V\,s^{-1}}$ of increase of the applied voltage.

can be obtained combining equation (19) with probability of the breakdown in the time interval $(t, t + dt)$ given by

$$f(t)\,dt = Y(t)\,W(t)\exp\left(-\int_0^{t-t_f} Y(t')W(t')\,dt'\right)dt, \quad (20)$$

which is written for constant t_f, yielding

$$f(U) = \frac{Y\,W(U)}{k}\exp\left(-\int_{U_s}^{U-kt_f}\frac{Y\,W(U_w)}{k}dU_w\right), \quad (21)$$

where constant Y is assumed. To obtain a final expression for $f(U)$ it is necessary to calculate integral in (21), and equation (3) should be combined with some $q(U_w)$ dependence. Assuming [10, 13]

$$q(U_w) = \gamma\left[\left(1+\frac{1}{\gamma}\right)^{U_w/U_s} - 1\right] = \gamma[\exp(\eta U_w) - 1], \quad (22)$$

it follows that

$$f(U) = \frac{YW}{k}\exp\left\{\frac{Y}{k}\left[\frac{1}{\gamma\eta}\ln\left(\frac{1-\exp(-\eta(U-kt_f))}{1-\exp(-\eta U_s)}\right) - (U - kt_f - U_s)\right]\right\}. \quad (23)$$

Distribution (23), with a slight difference due to different integral boundaries, was reported in [23].

The integration in (21) can be approximated assuming linear dependence $W(U_w)$, which yields

$$f(U) = \frac{YW(U)}{k}\exp\left[-\frac{YW(U)}{2k}(U - kt_f - U_s)\right] \quad (24)$$

as reported in [24] (with $t_f = 0$).

Figure 2 shows the comparison of two density functions (equations (23) and (24)) with data recorded in nitrogen-filled tube ($p = 4.0$ mbar) with spherical iron electrodes and $k = 50\,\mathrm{V\,s^{-1}}$, shown with dots. The curve that represents (23) was firstly obtained using fitting procedure where Y/k, γ and t_f were assumed as the fitting parameters. The curves that correspond to (24) are plotted with the same Y/k, γ and t_f previously determined for equation (23), and also for the case of $t_f = 0$. Figure 2 shows very similar shapes of the complete distribution (equation (23)) and simplified distribution (equation (24)). Future investigations will concentrate on improvement of the breakdown voltage ditribution density, in order to get a more precise but still simple function.

3. Methods for determination of static breakdown voltage

There are several methods for estimation of the static breakdown voltage U_s. Two methods normally used in our laboratories will be considered here [15, 16, 25]. The breakdown cease method will be described first. In this method, the voltage is applied to the tube and the tube is moved towards the breakdown status. After that, U_w is swiched off and on during each second, decreasing the U_w value simultaneously. The minimum voltage value for which the electrical breakdown still appears can be considered as U_s.

Static breakdown voltage can also be estimated using dynamic method [24]. This method is based on the determination of $U_b = f(k)$, where U_b is the measured breakdown voltage and k is the rate of the increase of the applied voltage (see equation (19)). Due to linear ramp, k is in fact the ratio between the voltage step and the time interval between successive steps. The voltage step was 1 V, while the time interval was varied from 0.01 to 1 s, and, consequnetly, the obtained values of k were from $100\,\mathrm{V\,s^{-1}}$ to $1\,\mathrm{V\,s^{-1}}$. Extrapolation of the $U_b = f(k)$ dependence to the intersect with U_b-axis (for $k = 0$) gives the estimation of U_s. This method has been used for nitrogen-filled tube at 4.0 mbar and results are shown in figure 3 for k values from 1 to $12\,\mathrm{V\,s^{-1}}$. Points in the diagram represent mean values for 100 measurements of U_b and $U_b = f(k)$ has been fitted by third order polynomial and estimated U_s value was ≈390 V.

The estimated U_s value depends on the k values for which the fit was done. Larger k values give higher U_s value. This can be observed by comparing the results in figures 3 and 4. As can be seen from figure 4, estimated U_s value for k values from 10 to $100\,\mathrm{V\,s^{-1}}$ is ≈414 V. It can be concluded that estimation of U_s will be more precise if k values for determination of $f(k)$ dependence are lower.

As previously mentioned, U_s depends on several parameters. For instance, our investigations have shown that U_s depends on the cathode material (U_s is lower for gold than for copper cathode) [24], and on irradiation presence (U_s is lower when the tube is irradiated by γ-rays). The latter is in accordance with an earlier result that had shown that additional ionization in interelectrode space decreases the breakdown voltage [26].

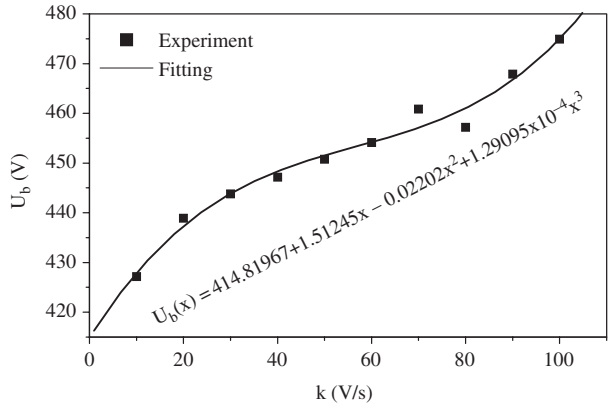

Figure 4. Breakdown voltage U_b as a function of the rate $k = 10$–$100\,\mathrm{V\,s^{-1}}$ of increase of the applied voltage.

4. Analysis of time delay

The exponential distribution for time delay was historically established as the Laue distribution. The $R(t)$ (equation (16)) can be replaced (in a statistical manner) as

$$R(t) = \frac{n(t)}{N} = \exp\left[-\frac{t - t_f}{\bar{t_s}}\right], \tag{25}$$

where $n(t)$ is the number of t_d values greater than actual time t, and N is the total number of measured t_d values. It is obvious that equation (25) enables appropriate visual interpretation of time delay distribution. Namely, plot of $\ln(n/N)$ vs t represents linear graph, known as Lauegram, and formula (25) is known as Laue distribution [1], after the pioneering work of von Laue [8].

The points of Lauegram obtained on the basis of t_d measurements enable estimations of t_f and $\bar{t_s}$. If the linear graph is fitted through these points using some best fit method (e.g. least-squares method), $\bar{t_s}$ determines the slope of $\ln(n/N)$ vs t, while t_f can be estimated from the intersection of that graph with the time axis. To obtain an adequate accuracy in evaluation of $\bar{t_s}$ and t_f, N must be large, as the accuracy increases as $\sqrt{1/N}$ [1].

Figure 5 shows the Laue distributions of 1000 t_d values for afterglow periods from 0.3 to 3 s and overvoltage of 6% for nitrogen-filled tube at 1.3 mbar [27]. Fittings are obtained by the least-square method. The insignificant discrepancy of experimental points from straight lines in figure 5(*b*) indicates the validity of Laue distribution. The same conclusion may be made for the results shown in figure 5(*a*), but the observed knees of the experimental points for small values of t_d could create suspicion. To explore this question, it is useful to plot histograms and fitted corresponding distribution density. This is shown in figure 6 for three values of the relaxation time τ. Fittings have been done in a manner that t_f in equation (25) has been estimated as $t_{d\,min}$, and after that $\bar{t_s}$ obtained from the least-squares fit of the function $1 - F(t_d - t_{d\,min})$. The results in figure 6 show the validity of t_d exponential distribution for $\tau = 1$ s, since the exponential distribution density very precisely fits t_d histogram. On the other hand, for $\tau = 0.3$ and 0.5 s, exponential distribution for t_d does not hold, meaning that a group of lower t_d values significantly disturbs the exponential

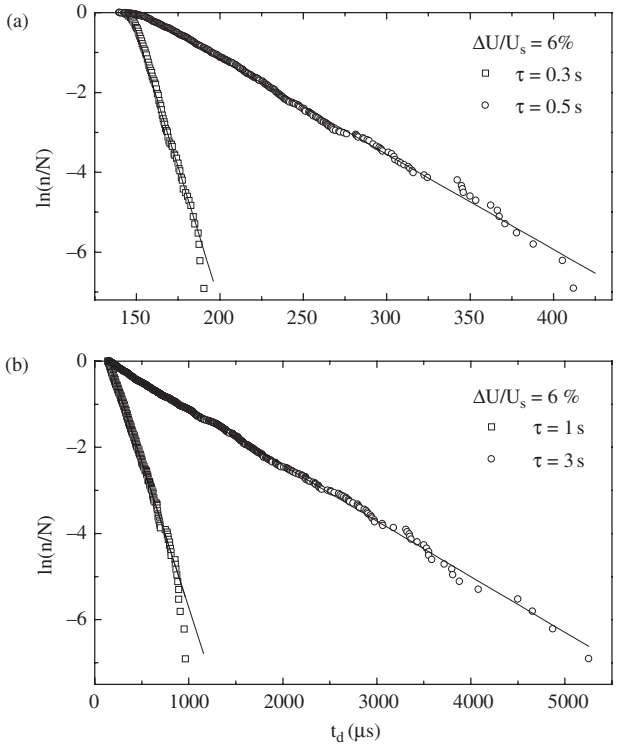

Figure 5. Laue distributions of time delay for four different values of afterglow period for nitrogen-filled tube at pressure 1.3 mbar [27] (©1998 IEEE).

distribution. This cannot be clearly seen from Lauegram (figure 5(*a*)), where only a slight discrepancy from the fitted line in the low t area can be observed. The reason for the disturbance of exponential distribution is the fact that $\tau = 0.5$ s and $\tau = 0.3$ s lie in the transitional region (ii), where the physical mechanism for breakdown initiation starts to change.

Equation (18) shows that formative time can be estimated as

$$t_f = \bar{t_d} - \sigma. \tag{26}$$

This estimation method is known as a moment method. Besides the moment method, there are two additional methods for t_f estimation: from Lauegram, and as a minimum t_d value in the set of measured values.

The moment method is based on the fact that shifted exponential distribution (14) is strongly asymmetrically and monotonically decreased, and, consequently, $\lim_{N\to\infty} \epsilon = 0$, where $\epsilon = t_{d\,min} - t_f$. Figure 7 shows the comparison of the three different estimation methods of formative time, showing t_f vs τ [28]. It can be seen that for small τ, t_f estimated from Lauegram deviates from those obtained by other two methods. Such behaviour is expected, since for small τ, t_d lies in areas (i) and (ii), where exponential distribution for t_d is not valid. An agreement of moment method estimation with minimum value could be attributed to the fact that in these areas σ is very small. For higher τ, shifted exponential distribution for t_d is established and moment method and Lauegram t_f estimations give approximately the same results, different from the minimum value. Since change of formative time with the increase of τ is not expected, it can be concluded that those two estimations become rough, and therefore unreliable.

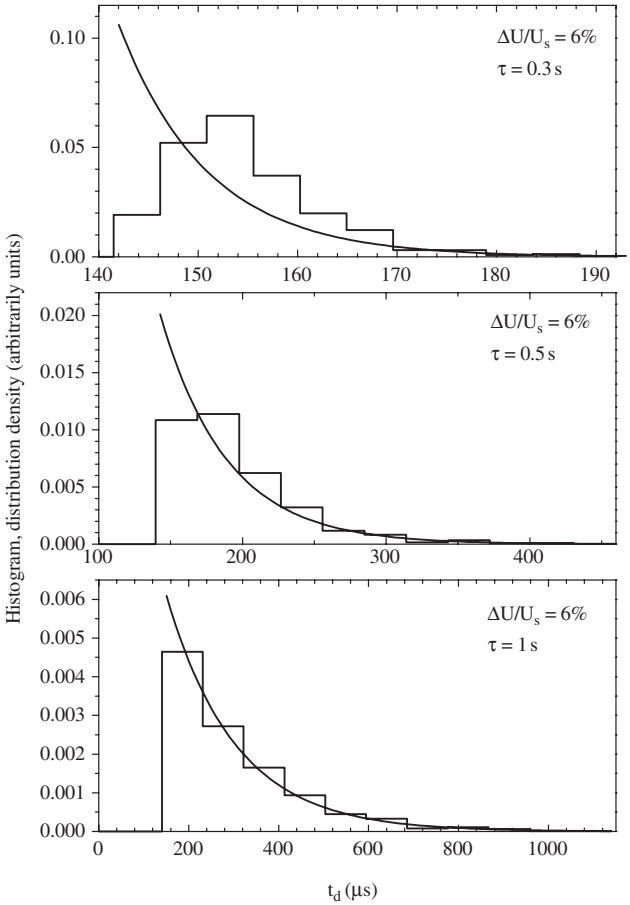

Figure 6. Histograms and fitted distribution densities of time delay for three different afterglow periods for nitrogen-filled tube at pressure 1.3 mbar [27] (©1998 IEEE).

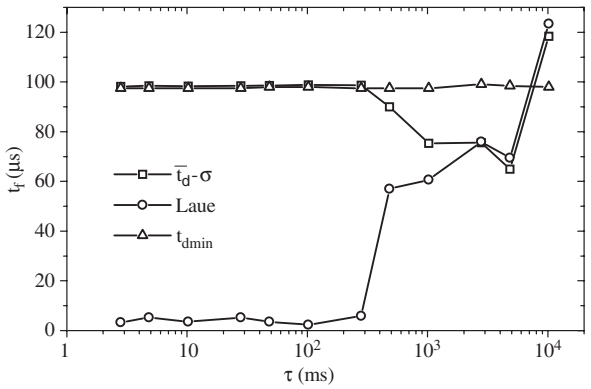

Figure 7. Formative time t_f as a function of afterglow period τ for nitrogen-filled tube at pressure 1.3 mbar [28].

The breakdown probability W can also be estimated from the time delay measurements. If $\bar{t_d}$ saturates with the increase of applied voltage, considering that it is a consequence of saturation of W, and if a voltage independent Y is assumed, then, neglecting t_f in (17), it follows [29, 30] that

$$W\left(\frac{\Delta U}{U_s}\right) = \frac{\bar{t}_{d\,sat}}{\bar{t_d}(\Delta U/U_s)}, \qquad (27)$$

where $\bar{t}_{d\,sat}$ is the saturation value of $\bar{t_d}$. This estimation

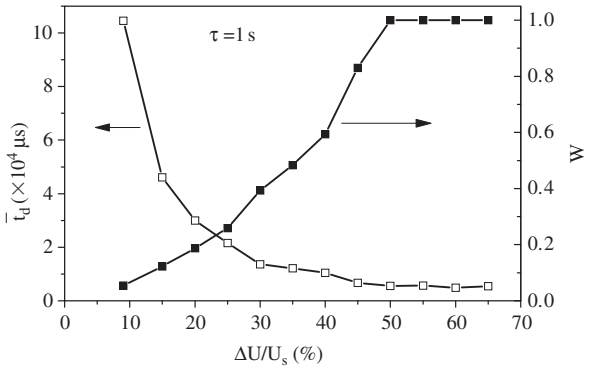

Figure 8. Mean value of time delay $\bar{t_d}$ and breakdown probability W as a function of overvoltage for kripton-filled tube at presssure 2.7 mbar [31].

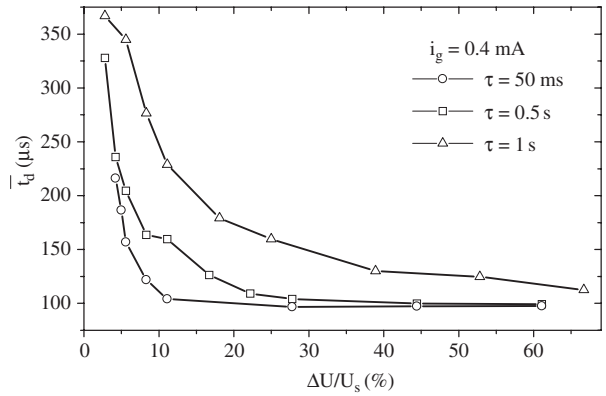

Figure 9. Mean value of time delay $\bar{t_d}$ as a function of overvoltage $\Delta U/U_s$ for three different values of afterglow period for nitrogen-filled tube at pressure 1.3 mbar [27] (©1998 IEEE).

obtained for krypton-filled tube with pressure $p = 2.7$ mbar is shown in figure 8 [31]. It is worth noting that this estimation for W is restricted to the area where W is close to unity. If $W \ll 1$, the assumption of independent avalanches starts to fail and the whole model described by equation (13) becomes questionable [22].

4.1. Influence of different experimental parameters on time delay

The time delay depends on many experimental parameters. One of the most important is the voltage applied on the tube electrodes U_w. Instead of applied voltage U_w, sometimes it is more convinient to deal with overvoltage (in percentage) $\Delta U/U_s \times 100\%$, where ΔU is defined as $\Delta U = U_w - U_s$.

The $\bar{t_d}$ vs $\Delta U/U_s$ dependence for nitrogen at pressure of 1.3 mbar and afterglow periods of 50 ms, 0.5 s and 1 s, are given in figure 9 [27], showing that this dependence exhibits monotonic decreasing behaviour. The decrease of the particular curve in figure 9 can be explained in a different way. For $\tau = 50$ ms, the SEE is dominantly induced by positive ions (see next section), and Y is large enough to give $t_s \ll t_f \to t_d \approx t_f$. Higher $\bar{t_d}$ (i.e. t_f) values for low overvoltage values can be attributed to lower values of electron ionization coefficient α. As the overvoltage increases, the electrons get

a greater amount of kinetic energy between the collisions, and their ionization coefficient increases exponentially [6], so that t_f falls to its minimum value. In the case of lower electron ionization coefficient, t_f depends on the rate of electrons that produce avalanche. This can be seen in figure 10 [27], where the $\bar{t_d}$ curves are shown as a function of overvoltage $\Delta U/U_s$ for two values of glow current and $\tau = 50$ ms. Namely, higher glow current produces higher ion number density and, consequently, Y increases, decreasing t_d.

For $\tau = 1$ s (figure 9), the positive ions have been recombined, Y is reduced, and the corresponding decreasing curve is a consequence of the increase of probability for an electron to cause the breakdown (W) through the whole overvoltage range, as well as the increase of ionization coefficient for low voltage values [27]. For $\tau = 0.5$ s, the value of Y is not large enough to produce $t_d \approx t_f$ itself, but this condition is reached with the increase of overvoltage when W also increases.

The effect of illumination by nitrogen-filled lamps on the $\bar{t_d} = f(\Delta U/U_s)$ dependence for the nitrogen-filled tube at 1.3 mbar is shown in figure 11 [32]. The $\bar{t_d}$ values are considerably smaller in the case with illumination than in the case without it, for all values of overvoltage. This is opposite to the results obtained in [33], where it was shown that the time delay was greater with illumination. Our investigations have shown [32] that the light from the lamp does not influence the active states created in the gas during the discharge (i.e. the quenching of $N_2(A^3\Sigma_u^+)$ states) as was concluded in [33, 34], but that the light induces the production of additional secondary electrons from the cathode in the photoemission process. These released electrons increase the probability of breakdown in gas, leading to a decrease of time delay for the same values of overvoltage.

The next investigated parameter that influences t_d is the electrode material. $\bar{t_d}$ as a function of the difference between the applied voltage and the static breakdown voltage ($U_w - U_s$) for nitrogen-filled tubes with different electrode materials ($p = 7$ mbar, $\tau = 10$ s) is shown in figure 12 [35]. The results obtained confirm that $\bar{t_d}$ value increases with the increase of electrode material work function for a given value of $U_w - U_s$ as a consequence of Y lowering (the work functions of Al, Pb and Mo are 3.74, 4.02 and 4.63 eV, respectively [36]).

The $\bar{t_d}$ and U_s depend on cathode surface quality (flatness and purity). This can be observed on the basis of cathode surface conditioning by the large number of successive breakdowns, for which t_d values are measured [37, 38]. The results are shown in figure 13 for the nitrogen-filled tube at a pressure of 97.5 mbar, 20% overvoltage and $\tau = 10$ s [39]. Each point in the $\bar{t_d} = f(N)$ curve represents $\bar{t_d}$ obtained after

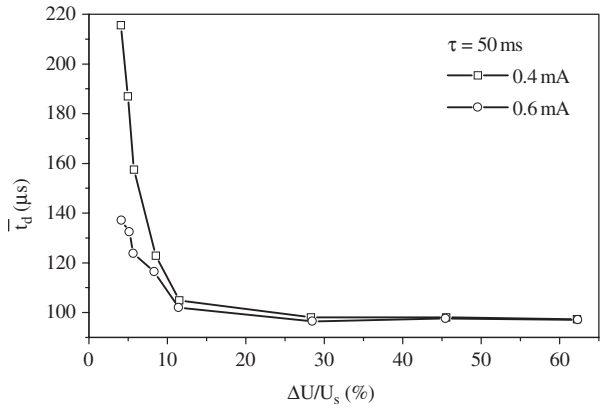

Figure 10. Mean value of time delay $\bar{t_d}$ as a function of overvoltage $\Delta U/U_s$ for two different values of glow current for nitrogen-filled tube at pressure 1.3 mbar [27] (©1998 IEEE).

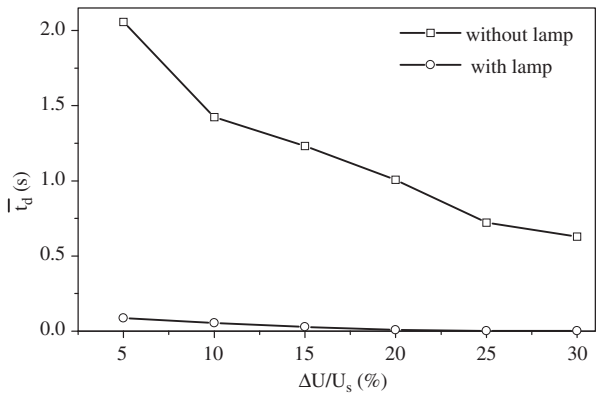

Figure 11. Mean value of time delay $\bar{t_d}$ as a function of overvoltage $\Delta U/U_s$ for nitrogen-filled tube at pressure 1.3 mbar in the cases with/without illumination lamps [32].

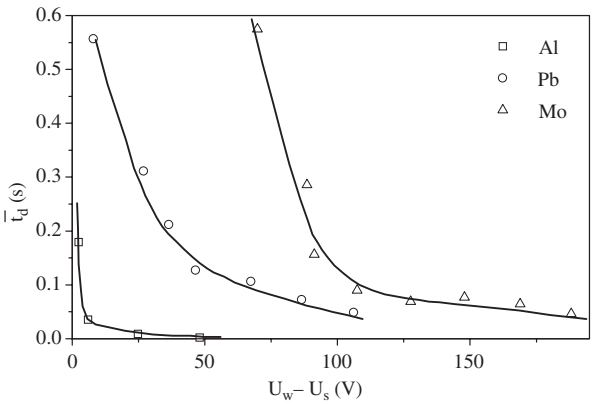

Figure 12. Mean value of time delay $\bar{t_d}$ as a function of difference between the applied voltage and the static breakdown voltage $U_w - U_s$ for nitrogen-filled tube at pressure 7.0 mbar with three pairs of electrodes made of Al, Pb and Mo [35].

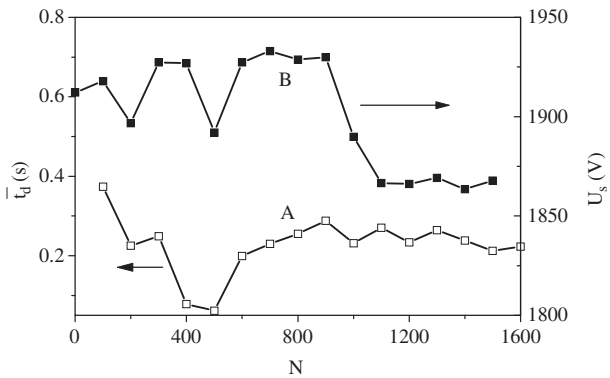

Figure 13. Mean value of time delay $\bar{t_d}$ and static breakdown voltage U_s as a function of a number of breakdowns N for nitrogen-filled tube at pressure 97.5 mbar. (A) $\bar{t_d} = f(N)$, $\tau = 10$ s; (B) $U_s = \varphi(N)$ [39].

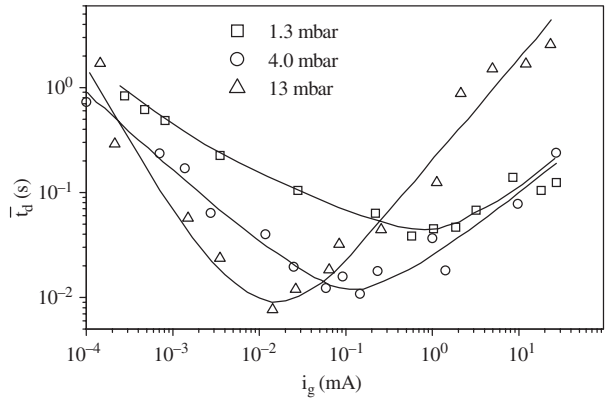

Figure 14. Mean value of time delay $\bar{t_d}$ as a function of glow current i_g for three nitrogen-filled tubes with different pressures [40].

each series of 100 successive breakdowns. After each 100 electrical breakdowns, the U_s measurements were repeated, and $U_s = f(N)$ dependence is also shown in the same figure. It can be seen that the fluctuations in t_d and U_s were higher for $N < 1000$ than for $N > 1000$, meaning that the cathode conditioning cleaned the cathode surface and made SEE approximately constant.

The influence of glow current i_g on $\bar{t_d}$ in nitrogen-filled tubes at pressures of 1.3, 4.0 and 13 mbar, and $\tau = 10$ s is shown in figure 14 [40]. $\bar{t_d}$ initially decreases with i_g, passing through a minimum, and then begins to increase. The i_g value for which the minimum of $\bar{t_d} = f(i_g)$ curves appears decreases with the decrease of gas pressure in the tube, occurring at $i_g \approx 14$, 140 and 1050 μA for $p = 1.3$, 4.0 and 13 mbar, respectively. It can also be noticed that the curve minima move towards higher $\bar{t_d}$ values with increase of the pressure. The appearance of minima in these curves indicates the existence of optimum value of i_g that corresponds to the maximum number density of neutral active states created during the discharge.

5. Memory curves

One of the most important parameters that influences $\bar{t_d}$ is the afterglow period τ. The studious investigations on this topic have been performed in Niš for more than 40 years, initially in the Electronic Industry Ltd., and later at the Faculty of Electrical Engineering, University of Niš. The $\bar{t_d} = f(\tau)$ dependence (memory curves) have been used for the qualitative analysis of recombination times and deexcitation times of the positive ions and neutral active states, respectively, formed during the previous breakdown and discharge. Thus, after the applied voltage is switched off, the concentrations of these particles decrease during the afterglow period due to their recombination on the tube walls, electrodes and in gas volume. The rates of these processes depend on the gas pressure as well as on tube volume and tube geometry. The particles which come to the cathode play the main role in the initiation of subsequent breakdown. They induce the SEE and if the voltage applied on the electrodes is higher than the static breakdown voltage, secondary electrons created at the cathode can initiate the subsequent breakdown. Since the SEE probability depends on concentrations of created particles in gas during the breakdown and discharge (especially neutral active states) these concentrations directly influence t_d. The concentration of particles created in gas decreases with τ, leading to the t_d increase.

The first memory curves, recorded for hydrogen, some noble gases and air at low pressure and for τ from 5 s to 24 h have been reported in [25, 41]. The curve saturation was shown to occur for τ from one the to few hours, depending on the gas type and pressure. The memory curves for He, Ar, Kr and Xe at 13 mbar and for τ from 1 s to 24 h were presented in [42], showing that τ values for which the saturation occurred depend on the pressure but do not exceed few hundred seconds. Later investigations were performed for τ from $\sim$1 ms up to 24 h [43], recorded in nitrogen at a pressure of 1.3 and 13 mbar as well as in He and Kr at 13 mbar. These results enabled observation of the presence of positive ions, the recombination time of which is much shorter than recombination and deexcitation times of the neutral active states, in the afterglow period.

Recently, our extensive investigations have been concentrated on the development of a method for the determination of the positive ion recombination times, atom recombination times for molecular gases and deexcitation times for metastable states in noble gases, all created during the breakdown and following discharge. The analysis of these processes has been done by memory curves recorded with strictly defined parameters, such as the afterglow period, glow current and time, and overvoltage. For this purpose, the system for automatic measurements of time delay and data aquisition has been designed and realized [44]. This system consists of three subsystems: (1) voltage supply and sense subsystem, (2) analog relaxation time setting subsystem and (3) digital control and measurement subsystem. The voltage supply and sense subsystem is composed of (a) regulated DC power supply at 100–1000 V and 20 mA, (b) steady-state current regulation resistors and (c) sensor resistor for the selection of the appropriate start–stop measuring level. The digital control and measurement subsystem comprises a PC with an ED 2000 data aquisition card under the control of a C program (see [44] for details).

In the following text, the memory curves recorded with the system described above for gas-filled molybdenum glass tubes with the spherical electrodes made of Fe, Cu and Au (the shape of the tube is given in [45]) will be shown. Before the gas was admitted, the tubes were baked out at 350°C and evacuated to a pressure of 10^{-7} mbar in a process similar to that for production of x-ray and other electron tubes. The tubes were then filled with Matheson research grade gases (N_2, H_2, Ar or Kr) at different pressures (oxygen impurity content was less than 1 ppm). Before the static breakdown voltages were determined, the cathode sputtering with glow current of $i_g = 0.5$ mA was set with duration of a few hours. The values of the static breakdown voltages were determined as described in [24]. Due to stochastic nature of t_d, each point in memory curves represents the mean value of 100 measured time delay values. After the breakdown, the current in the tube (glow current) was $i_g = 0.5$ mA during a glow time $t_g = 1$ s (see the time cycle in [31] for details). This time was sufficient to establish saturation of ion and neutral active state concentrations in the tube.

The memory curves for three geometricaly identical nitrogen-filled tubes with Fe electrodes at pressures of 0.67,

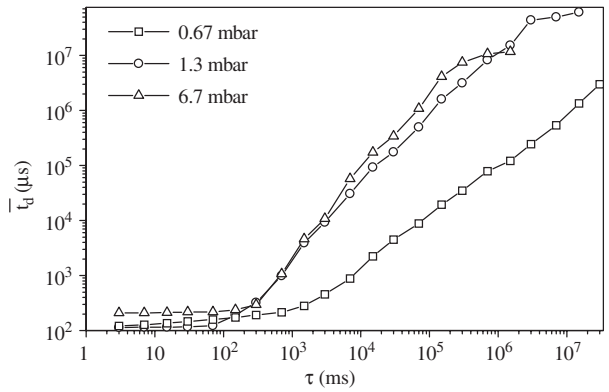

Figure 15. Memory curves for three nitrogen-filled tubes with different pressures.

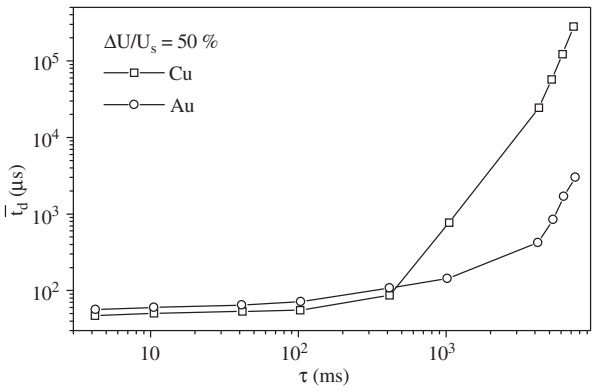

Figure 16. Memory curves for Cu and Au cathode for nitrogen-filled tube at pressure 6.7 mbar [57].

1.3 and 6.7 mbar and 50% overvoltage are shown in figure 15. All three curves have plateaus up to τ value of about 200 ms (for these τ values, $\bar{t_d}$ changes insignificantly with τ). For τ values greater than 200 ms, $\bar{t_d}$ increases with τ and for pressure of 6.7 mbar memory curve reaches saturation for $\tau \approx 700$ s. For pressure of 1.3 mbar, the curve saturation occurs for τ that is one order of magnitude greater while, for pressure of 0.67 mbar, saturation does not appear even for $\tau = 8$ h.

The shapes of the memory curves in figure 15 can be explained on the basis of the recombinations of the positive ions and atoms, and the deexcitation of metastable states, remaining from previous breakdown and discharge, as well as cosmic rays present. Thus, the curve plateaus for the small values of τ are a consequence of the presence of positive ions in the gas. Since the ions have high drift velocities and reach the cathode almost instantly after the application of the voltage, releasing the secondary electrons (Auger electrons), the breakdown probability is almost independent of the ion concentration and t_d values are small. In this case, the production of electrons is very high and the time delay is approximately equal to the formative time ($t_d \approx t_f$). For small τ values, the considerable concentration of N atoms and N_2 ($A\,^3\Sigma_u^+$) metastable states are also present but, due to their electrical neutrality their role in SEE is negligible in comparison with the role of positive ions. On the basis of this region, the recombination time of ions can thus be determined as the plateau length. In this particular case of nitrogen-filled tube it is ∼200 ms.

After the positive ion recombination, the nitrogen atoms remaining from the previous discharge, the effective lifetime of which is longer than 1 h [46], play a dominant role in the SEE. Thus, part of these atoms recombines at the cathode by catalytic recombination processes, giving N_2 ($A\,^3\Sigma_u^+$) metastable states which produce secondary electrons [29, 47, 48]. If the voltage is applied, these electrons can cause the electrical breakdown. It should be emphasized that a significant concentration of N_2 ($A\,^3\Sigma_u^+$) metastable states is generated in gas during the breakdown and following discharge [49]. Meanwhile, many investigations have shown that the effective lifetime of these states can be efficiently quenched in collisions with nitrogen atoms [50], other N_2 ($A\,^3\Sigma_u^+$) metastable states (reaction of energy pooling, resulting in N_2 $B\,^3\Pi_g$ and N_2 $C\,^3\Pi_u$ [51,52]), neutral molecules [53], as well as with tube [54]. Else, the N_2 ($A\,^3\Sigma_u^+$) metastable state has a very short effective lifetime (of the order of milliseconds [30,55]) and cannot influence the breakdown in late afterglow periods.

As τ increases, the concentration of nitrogen atoms decreases. Since $t_s \gg t_f$, $\bar{t_d}$ can be expressed as $\bar{t_d} \approx 1/(YW)$ (see equation (17)). Y depends on the concentration of N atoms remaining in the afterglow period (Y increases with the concentration of N atoms), while W depends on the overvoltage (W increases with voltage). Since $W = \text{const}$ for a given overvoltage value, $\bar{t_d}$ must increase with increase of the afterglow period, which is confirmed in figure 15. The lowering of the saturation onset with the pressure increase in figure 15 is a consequence of a smaller initial concentration of N atoms and their faster volume recombination (reactions are given in [56]).

The saturation of the memory curve for pressure of 6.7 mbar is a consequence of the significant decrease of N atoms that decreases the probability for the SEE. Hence, the breakdown is initiated by cosmic rays. Since the flux of cosmic rays varies insignificantly, $\bar{t_d}$ values are approximately constant. For the nitrogen-filled tube at 0.67 mbar pressure, saturation does not occur even for $\tau \approx 8$ h. This shows that N atom concentration is still significant and the influence of cosmic rays is not important yet.

On the basis of the memory curve saturation (figure 15), the recombination times of N atoms for various nitrogen pressures can be estimated, and these values are ∼700 s, 3×10^3 s and $>3 \times 10^4$ s for pressures of 6.7, 1.3 and 0.67 mbar, respectively, showing the strict lifetime dependence on the pressure.

A very important parameter which affects the shape of the memory curve is the cathode material. The memory curves for nitrogen-filled tube at 6.7 mbar and 50% overvoltage, with Cu and Au cathodes are presented in figure 16 [57], showing that the curves have plateaus up to $\tau = 400$ ms. The SEE is induced by the positive ions in this τ region, and t_d changes very slightly. For $\tau \geqslant 400$ ms, there are no positive ions, and the SEE is induced by N atoms, while the influence of the nitrogen metastable states on the electrical breakdown can be neglected. In this case, $\bar{t_d}$ values are higher for Cu than for Au electrode, and this difference can be explained by different adsorption ability of cathode materials, according to the adsorption model in [58]. Namely, the adsorbed layer of N atoms covered by a pseudo-layer of N_2 molecules is formed at the metal surface, decreasing the probability of SEE through absorbed layers.

Since N atoms are more adsorbed on Cu, the probability of secondary emission from Cu is considerably smaller than the one from Au plated cathode.

It is worth noting that the results shown in figure 16 are in good agreement with our previous results [59] for the tubes with Au and Cu electrodes, which were also filled by nitrogen, but at pressure of 13 mbar. Memory curves were recorded in τ range of 5–300 s, i.e. in the region when SEE is initiated by N atoms remaining from previous breakdown and discharge.

On the basis of the memory curves numerical modelling of the kinetics of neutral active states (such as N atoms and N_2 ($A^3\Sigma_u^+$) metastable states) has been performed [29, 48, 55, 60–65]. Partial differential equations containing the terms that correspond to concentration decay in gas, on the tube walls and electrodes have been employed. The results show that this method can successfully model parts of the memory curve which lie immediately after the positive ion recombination, i.e. in τ interval from few hundreds of milliseconds up to 10 s.

The afterglow periods for both the plateau ending and the saturation of memory curves depend on the gas type. This can be observed from figure 17 for N_2 and H_2 [66] and figure 18 for Ar and Ne (in all cases the pressure was 6.7 mbar and overvoltage 50%). Figure 17 shows that the plateau length for nitrogen memory curve is two orders of magnitude smaller than the plateau length for hydrogen memory curve. This means that the same conclusion is valid for the corresponding positive ions' recombination times. The saturation of nitrogen curve occurs for a τ value which is an order of magnitude smaller than for the corresponding hydrogen curve, leading to the conclusion that N atom recombination time also has a similar relation to H atom recombination time, which is in good agreement with literature data [67].

The plateaus in Ar and Ne curves (figure 18) practically do not exist, implying that their ion recombination times are <3 ms. On the basis of a memory curve saturation, it can be concluded that deexcitation time of metastable states in Ar is about an order of magnitude shorter than in Ne (in noble gases metastable states are $^3P_0$ and $^3P_2$). Estimated values of the metastable state deexcitation times in Ar and Ne (figure 18) are ≈60 and ≈300 s, respectively, which is in good agreement with theoretical results [68]. The experimental results for the metastable state deexcitation times in Ar and Ne obtained by the time-of-flight technique are >1.33 and >0.8 s, respectively [69].

The influence of the overvoltage on memory curves can be observed in figure 19 [31]. The curves are recorded for Kr at 2.7 mbar pressure and overvoltages of 16%, 50% and 100%. It can be seen that the increase of overvoltage leads to a decrease of t_d for a given τ value, while the saturation occurs for approximately the same τ values of ≈100 s. These results confirm our previous conclusions given for nitrogen memory curves that Y decreases with afterglow period, while the breakdown probability W increases with the overvoltage. Since Y = const for a given τ, it follows from equation (17) that $\bar{t_d} \sim 1/W$, assuming $t_f \ll t_s$. Very similar behaviour of memory curves was obtained for Ar [70].

The τ value for which the memory curve reaches saturation decreases when the tube is irradiated by photons with sufficient energy to pass through the glass and release electrons from the cathode (Compton electrons) or produce gas ionization (the latter effect has a smaller probability due to low gas pressure—low gas particle concentration). The influence of γ-photons from external radioactive source, ^{60}Co, on the memory curve for nitrogen-filled tube at pressure of 1.3 mbar and overvoltage of 50% are shown in figure 20 [71]. The curves correspond to exposed dose rates of $RD_{e1} = 2.1 \times 10^{-11}$ C kg^{-1} s^{-1} and $RD_{e2} = 6.5 \times 10^{-10}$ C kg^{-1} s^{-1}, as well as to the case without irradiation $RD_{e0} = 0$. Figure 19 shows that for relatively small τ values, when positive ions and significant N atom concentration exist, the Compton

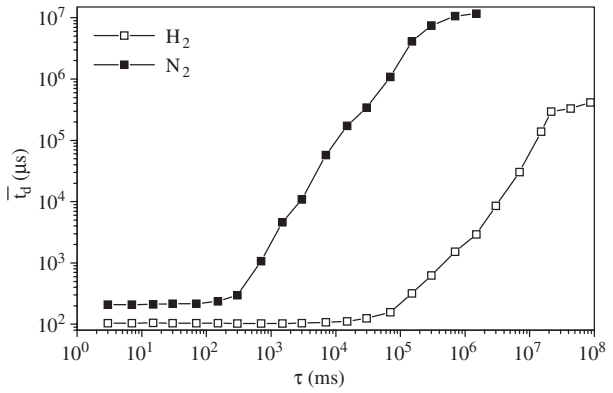

Figure 17. Memory curves for hydrogen-filled tube and nitrogen-filled tube at pressure 6.7 mbar [66].

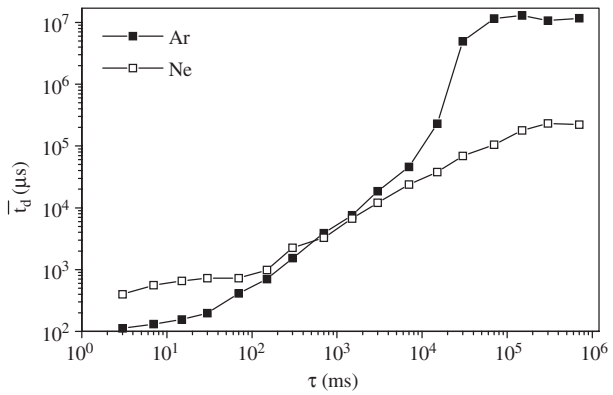

Figure 18. Memory curves for argon-filled tube and neon-filled tube at pressure 6.7 mbar.

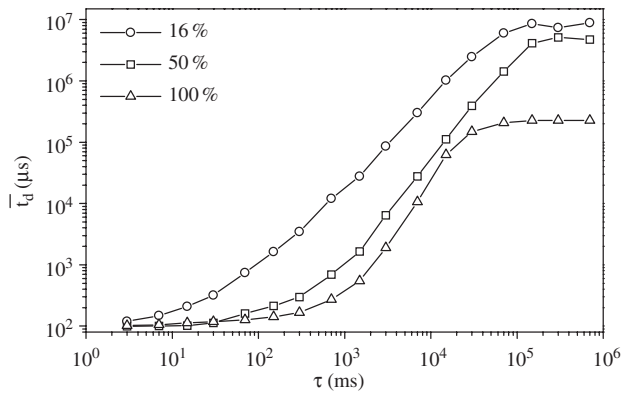

Figure 19. Memory curves for three different values of overvoltage for krypton-filled tube at pressure 2.7 mbar [31].

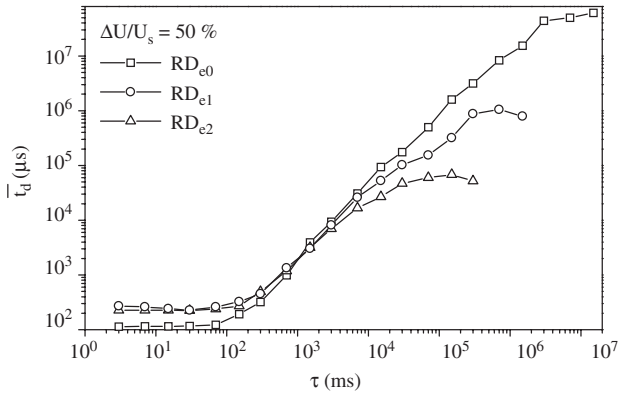

Figure 20. Memory curves for krypton-filled tube at pressure 1.3 mbar without irradiation and two values of irradiation dose rate [71].

electrons [72] released from the cathode by external radiation have no significant influence on the SEE. For $\tau > 6$ s, clear differences in $\bar{t_d}$ values appear, and the influence of radiation can be separated. Thus, there are no positive ions and the concentration of N atoms is significantly decreased, so that the Compton electrons begin to dominate in the breakdown initiation. In the case without radiation, the saturation begins for $\tau \approx 3000$ s, and after that the breakdown is caused by electrons created by cosmic rays, since the concentration of N atoms is significantly decreased. In the case with radiation, for a given τ the $\bar{t_d}$ is greater for the smaller exposed dose RD_{e1}, because the SEE production in unit time is smaller than for RD_{e2}. For a given exposed dose rate the curve reaches saturation because the SEE production is approximately constant. Similar behaviour has been observed in Kr [31] and Ar [70].

6. Conclusions

Knowledge of physical processes that lead to electrical breakdown in gases is important for the operation of various gas devices, both those that need minimization of the static breakdown voltage, and those that should be kept in non-self-sustaining discharge, avoiding the breakdown. The SEE plays dominant role in initiation of electrical breakdown in low pressure gases (up to ≈10 mbar [2]), hence a theoretical analysis is performed on the basis of Townsend's theory. Many investigations have shown that an exact analysis can be performed on the basis of the experimental data of the breakdown voltage and time delay of electrical breakdown. These two mutually dependent random variables with certain distributions owe their stochastic character the statistical processes that occur in the gas volume, on the tube walls and electrodes.

Each gas tube has its own static breakdown voltage. Its proper definition requires the time delay: it is the highest voltage which keeps time delay infinitely long. There are many methods for estimation of the static breakdown voltage, but dynamic method is most often used.

Many previous investigations [11, 12, 73–75] have shown that the Laue distribution is valid for the t_d values that are of the order of a microsecond or a millisecond. Our numerous investigations imply that the validity of this distribution can be widen to the t_d data up to the order of 100 s [16, 43, 45, 76, 77]. The time delay distribution can also be considered by a Laue distribution and by histograms and corresponding probability density function for exponential distribution [27].

For the creation of the secondary electrons, indispensable for electrical breakdown initiation in low pressure gases, species remaining from previous breakdown and discharge play a dominant role. These species can be ions, which are created in all gases, and neutral active states, i.e. metastable states in noble gases, and both metastable states and atoms in molecular gases. In the literature, only the methods for detection of metastable states have been reported. The optical methods are the ones used most often and are based on absorption of light of a definite wavelength. These methods can be applied for high metastable state concentration ($>5 \times 10^6$ cm^{-3}) [78]. In the case of a lower metastable state concentrations it is more effective to detect secondary electrons created by metastable state interaction with metal surface [79]. According to the data given in [80], this method can be 10^8 times more sensitive than the optical methods. Results in [81] indicated the possibility of metastable state detection down to concentration of $\approx 10^4$ cm^{-3} measuring the electrical breakdown time delay.

Information about actual concentrations of the species remaining from a previous breakdown and discharge during the afterglow can also be obtained on the basis of the memory curves. This method enables the detection of charged and neutral species, i.e. ions, atoms and metastable states. The concentration of neutral active states can be monitored to very low values when the cosmic rays become responsible for the electrical breakdown initiation. Using this method the contributions of positive ions and neutral active states to the SEE can also be distinguished. The positive ion recombination times, catalytic atom recombination times and the metastable state deexcitation times can also be estimated using the memory curves. Memory curve also enables the detection of electons released from the cathode by γ-rays due to the Compton effect. This implies that gas tube can be used as a sensor of ionizing radiation [71].

References

[1] Meek J M and Craggs J D 1978 *Electrical Breakdown in Gases* (Chichester: Wiley)
[2] Razevig D V and Sokolova M V 1977 *Raschet nachal'nih i razryadnyh napryadzeniy gazovyh promedzutkov* (Moscow: Energia)
[3] Cobine J D 1958 *Gaseus Conductors: Theory and Engineering Applications* (New York: Dover)
[4] Von Engel A 1983 *Electrical Plasmas: Their Nature and Users* (New York: International Publications Service, Taylor and Frances)
[5] Gopanov B I 1960 *Electronika–Fizichekie osnovy* (Moscow: Gosudarstvenoe izdatelstvo Fiziko-matematicheskoy literatury)
[6] Von Engel A 1965 *Ionized Gases* (Oxford: Clarendon)
[7] Zuber K 1925 *Ann. Phys. Lpz.* **76** 231
[8] Von Laue M 1925 *Ann. Phys. Lpz.* **76** 261
[9] Loeb L B 1948 *Rev. Mod. Physik* **21** 151
[10] Wijsman R A 1949 *Phys. Rev.* **75** 833
[11] Llevellyn Jones F and de la Perrelle E T 1953 *Proc. R. Soc.* A **216** 267
[12] Morgan C G and Harcombe D 1953 *Proc. Phys. Soc.* B **66** 665

[13] Farquhar R L, Ray B and Swifft J D 1980 *J. Phys. D: Appl. Phys.* **13** 2067
[14] Bodareu E and Popescu I 1968 *Gaz Ionises (Decharge Electriques Dans les Gas)* (Paris: Dunom)
[15] Pejović M M 1980 *PhD Thesis* Faculty of Electronic Engineering, University of Niš, Yugoslavia
[16] Mijović B J 1985 *PhD Thesis* Faculty of Electronic Engineering, University of Niš, Yugoslavia
[17] Raizer Y P 1991 *Gas Discharge Physics* (Berlin: Springer)
[18] Meek J M and Craggs J D 1953 *Electrical Breakdown of Gases* (Oxford: Claredon)
[19] Bošan Dj A, Pejović M M and Vujović M V 1980 *Acta Phys. Acad. Sci. Hungar.* **49** 23
[20] Strigel R 1939 *Elektrische Stossfestigkeit* (Berlin: Springer)
[21] Pejović M M, Marković V Lj, Ristić G S and Mekić S 1996 *IEE Proc. Sci. Meas. Technol.* **143** 413
[22] Karamarković J P, Ristić G S and Pejović M M 2000 *Bulgarian J. Phys.* **27** 42
[23] Radović M, Jovanović T and Stepanović O 1997 *3rd General Conf. on the Balkan Physical Union (Cluj-Napoca, Romania, Proc. Suplement of Balkan Phys. Lett.* **5** *1443)*
[24] Pejović M M and Filipović R D 1989 *Int. J. Electron.* **67** 251
[25] Bošan Dj A 1976 *PhD Thesis* Faculty of Natural Science, University of Belgrade, Yugoslavia
[26] Filipović R 1987 *MSc Thesis* Faculty of Electronic Engeenering, University of Niš, Yugoslavia
[27] Pejović M M, Karamarković J P and Ristić G S 1998 *IEEE Trans. Plasma Sci.* **26** 1733
[28] Pejović M M, Karamarković J P, Ristić G S and Marković V Lj *Balkan Phys. Lett.* at press
[29] Marković V Lj 1993 *PhD Thesis* Faculty of Physics, University of Belgrade, Yugoslavia
[30] Marković V Lj, Petrović Z Lj and Pejović M M 1994 *J. Chem. Phys.* **100** 8514
[31] Pejović M M and Ristić G S 2000 *J. Phys. D: Appl. Phys.* **33** 2786
[32] Pejović M M, Ristić G S and Petrović Z Lj 1999 *J. Phys. D: Appl. Phys.* **32** 1489
[33] Bošan Dj A, Jovanović T V and Karmpotić Dj M 1997 *J. Phys. D: Appl. Phys.* **30** 3096
[34] Jovanović T V, Bošan Dj A and Krmpotić Dj M 1998 *J. Phys. D: Appl. Phys.* **31** 3249
[35] Pejović M M, Bošan Dj A and Krmpotić Dj M 1981 *Contr. Plasma Phys.* **21** 211
[36] Fomenko V S 1970 *Emissionnye Svoystva Materialov* (Kiev: Naukova Dumka)
[37] Simonović D 1983 *MSc Thesis* Faculty of Electronic Engineering, University of Niš, Yugoslavia
[38] Pejović M, Golubović S and Dimitrijević B 1984 *XXVII Yugosl. Conf. ETAN (Split, Yugoslavia)* p II229
[39] Pejović M M, Mijović B J and Bošan Dj A 1984 *J. Phys. D: Appl. Phys.* **17** 351
[40] Pejović M M and Dimitrijević B 1982 *J. Phys. D: Appl. Phys.* **15** L87
[41] Bošan Dj A 1978 *Proc. 5th Int. Conf. on Gas Discharges (Liverpool) IEE Conf. Publication* 165 (Stevenage: IEE) p 273
[42] Pejović M M, Mijović B J and Bošan Dj A 1983 *J. Phys. D: Appl. Phys.* **16** L149
[43] Pejović M M and Mijović B 1988 *Zh Tekh. Fiz.* **58** 2124 (Eng. Transl. *Sov. J. - Tech. Phys.* **33** 1290)
[44] Pejović M M, Ristić G S, Milosavljević Č S, Vuković P D and Karamarković J P 1999 *VACUUM—Surf. Eng., Surf. Instrum. Vac. Technol.* **53** 435
[45] Pejović M M, Bošan Dj A and Nikolić Z 1982 *J. Phys. D: Appl. Phys.* **15** 867
[46] Brenenen W and Shone E C 1971 *J. Phys. Chem.* **75** 1552
[47] Phelps A V *Personal comunication*
[48] Marković V Lj, Pejović M M and Petrović Z Lj 1993 *J. Phys. D: Appl. Phys.* **26** 1611
[49] Cernogora G, Hochard L, Touzeau M and Ferreira C M 1981 *J. Phys. B: At. Mol. Phys.* **14** 2977
[50] Young R A and John St G A 1968 *J Chem. Phys.* **48** 895
[51] Hays G N and Oskam H J 1973 *J. Chem. Phys.* **59** 1507
[52] Hays G N and Oskam H J 1973 *J. Chem. Phys.* **59** 6088
[53] Makabe T, Awai H and Mori T 1984 *J. Phys. D: Appl. Phys.* **17** 2367
[54] Piper L G 1989 *J. Chem. Phys.* **90** 7087
[55] Marković V Lj, Petrović Z Lj and Pejović M M 1995 *Japan. J. Appl. Phys.* **34** 2466
[56] Evenson K M and Burch D S 1966 *J. Chem. Phys.* **45** 2450
[57] Pejović M M, Marković V Lj, Ristić G S and Mekić S I 1997 *VACUUM—Surf. Eng., Surf. Instrum. Vac. Technol.* **48** 531
[58] Hays G N, Trasy C J and Oscam H J 1974 *J. Chem. Phys.* **60** 2027
[59] Pejović M M, Bošan Dj A and Nallbani B 1982 *J. Phys. D: Appl. Phys.* **15** L31
[60] Marković V LJ, Petrović Z Lj and Pejović M M 1996 *18th Summer School and Int. Symp. on the Physics of Ionized Gases (SPIG) (Kotor, Yugoslavia)* p 387
[61] Marković V Lj, Petrović Z Lj and Pejović M M 1996 *J. Phys. III France* **6** 959
[62] Marković V Lj, Pejović M M and Petrović Z Lj 1996 *Plasma Chem. Plasma Process.* **16** 195
[63] Marković V Lj, Petrović Z Lj and Pejović M M 1997 *Plasma Source Sci. Technol.* **6** 240
[64] Marković V Lj, Pejović M M and Petrović Z Lj 1997 *Int. Conf. Phen. in Ionized Gases* (Toulouse, France) IV-178
[65] Petrović Z Lj, Marković V Lj, Pejović M M and Gocić S R 2001 *J. Phys. D: Appl. Phys.* **34** 1756
[66] Pejović M M and Ristić G S 2001 *IEEE Trans. Plasma Sci.* submitted
[67] Smirnov B M 1974 *Ionoy i vozbudzennye atomy v plasma* (Moscow: Atomizdat)
[68] Samall-Warren N E and Lue-Yung Schaw Chin L Y 1975 *Phys. Rev.* A **11** 1777
[69] Van Dyck R S, Johnson Ch E and Shuoort H A 1972 *Phys. Rev.* A **5** 991
[70] Pejović M M and Ristić G S 2002 *Phys. Plasmas* **9** 364
[71] Pejović M M and Ristić G S 2000 *Rev. Sci. Instr.* **71** 2377
[72] Smirnov Yu M and Yudin N P 1980 *Yadarnaya fizika* (Moscow: Nauka)
[73] Llevellyn Jones F and Morgan C G 1953 *Proc. Roy. Soc.* A **218** 83
[74] Malcahy M J and Govinda Raju G R 1963 *9th Int. Conf. on Phen. in Ionized Gases (Bucharest)* p 226
[75] Nastase L 1976 *12th Int. Conf. on Phen. in Ionized Gases (Eindhoven)* p 93
[76] Pejović M M, Mijović B J and Bošan Dj A 1983 *J. Phys. D: Appl. Phys.* **16** 1953
[77] Mekić S I 1997 *PhD Thesis* Faculty of Natural Sciences University of Priština, Yugoslavia
[78] Bolden R C, Hemsworth R S, Shaw M J and Twiddy N D 1969 *Proc. 9th Int. Conf. on Phenomena in Ionized Gases (Bucharest)* p 27
[79] Martišovitš V and Košinar I 1973 *Proc. 11th Int. Conf. on Phenomena in Ionized Gases (Prague)* p 485
[80] Lancaster B M and Nygaard K J 1976 *12th Int. Conf. on Phenomena in Ionized Gases (Eindhoven)* p 91
[81] Lukashev A A and Chistyakov P N 1969 *9th Int. Conf. on Phenomena in Ionized Gases (Bucharest)* p 18